JOURNAL OF MATERIALS SCIENCE 24 (1989) 1291–1298

Effect of Ag on the electrical transport and iso-thermal transformation of amorphous As_2S_3

M. F. KOTKATA, C. S. MOHAMED
Physics Department, Faculty of Science, Ain Shams University, Cairo, Egypt

The step-wise technique is used to follow the possible changes in d.c. transport of three different glasses of the system Ag–As_2S_3 isothermally annealed at $T_g < T < T_m$. The isothermal time-dependence of different characteristic electrical quantities (e.g. E_σ, $\sigma_{20°C}$ and σ_0) has been drawn and correlated with the microstructural changes recorded for samples annealed at the same conditions. The effect of silver content (up to 25 at %) on the interplanar spacings (d_{hkl}) and relative intensities (I/I_0) of the diffraction lines of As_2S_3 illustrates that the structure of the three-component system Ag–As_2S_3 can be represented as a solid solution of an element (e.g. S), binary phases (e.g. AsS, As_2S_3), and/or ternary phases (e.g. $AgAs_2S_3$, $Ag_6As_2S_3$), depending on the concentration of silver in the composition.

1. Introduction

Arsenic sulphide, As_2S_3, is one of the most extensively studied chalcogenide semiconductors, it forms the most "stable" glass known and finds application in optical memory systems. This compound may be easily prepared in the glassy state, with a definite structure containing only As–S bonds. Such a glass has a comparatively narrow band gap. Unlike crystal, it apparently cannot depend on singly occupied donors or acceptors, though some impurities, namely those with less than four electrons outside a closed shell, shift the Fermi energy considerably, as may occur when copper, silver, gallium, indium or thallium are added to it [1, 2].

The inclusion of silver atoms in As_2S_3 has been investigated structurally [3]. It was found that silver atoms break up the As–S rings leading to early crystallization. The kinetics of photodissolution of silver into As_2S_3 is of interest because of imaging applications, and is determined by the rate of change of the electrical resistance of a thin silver layer during illumination [4].

Another application for the Ag–As–S system is in optical memory systems. It has been reported, in general, that glasses in which exothermic transformation occurs by slow heating have the characteristic of memory type, and some crystalline phases having low resistivity are formed after its reaction [5, 6]. Also, the construction and properties of As_2S_3–Ag film systems show their usefulness as hologram recording media [7].

In a previous paper [8], the effects of addition of silver (6 to 25 at %) on the d.c. conduction of amorphous As_2S_3 has been studied below the glass transition temperature, T_g. The results obtained were correlated with the variation of X-ray radial distribution function of the different glasses [8, 9].

The present work is aimed at studying the effect of isothermal-induced transformation on the electrical and structural characterization in three glasses of the chalcogenide ternary system $Ag_x(As_2S_3)_{100-x}$.

2. Experimental details

Three bulk glasses of the system $Ag_x(As_2S_3)_{100-x}$, with $x = 6$, 15, and 25, were prepared by heating mixtures from As_2S_3 glass rods and silver wires (both 99.999% pure) in vacuum-sealed (10^{-5} torr) fused silica ampoules at 700° C for 10 h during which the molten solution was occasionally shaken vigorously, then followed by ice-water quenching. X-ray diffraction (with Cu$K\alpha$ radiation on a vertical Philips diffractometer) and differential thermal analysis (DTA, Shimazo model DT-30) were used to identify the RDF structural changes and transition temperatures of the prepared glasses [8–10].

The fraction of a crystalline phase increases and that of the amorphous decreases when an appropriate heat treatment takes place. Therefore, in order to follow the change in electrical conduction during the crystallization process, a stepwise technique is considered. That is, the sample was subject to conduction for a given time at an isothermal temperature T ($T_g < T < T_m$), and then removed from the oven and subsequently quenched in cold air to stop the possible crystal growth in the sample. After that, the sample was polished to eliminate the effect of surface crystallization and the function $\sigma = f(T)$ was measured below T_g. The sample preparation for electrical conductivity (σ) and the measuring apparatus for X-ray diffraction, microstructure and d.c. conductivity were described in previous publications [8, 11, 12].

3. Results and discussion

3.1. Isothermal time-dependence of d.c. conduction

The d.c. electrical conductivity of the Ag–As_2S_3 glasses is exponentially dependent on $1/T$ and can be satisfactorily described below T_g by the thermally activated

0022–2461/89 $03.00 + .12

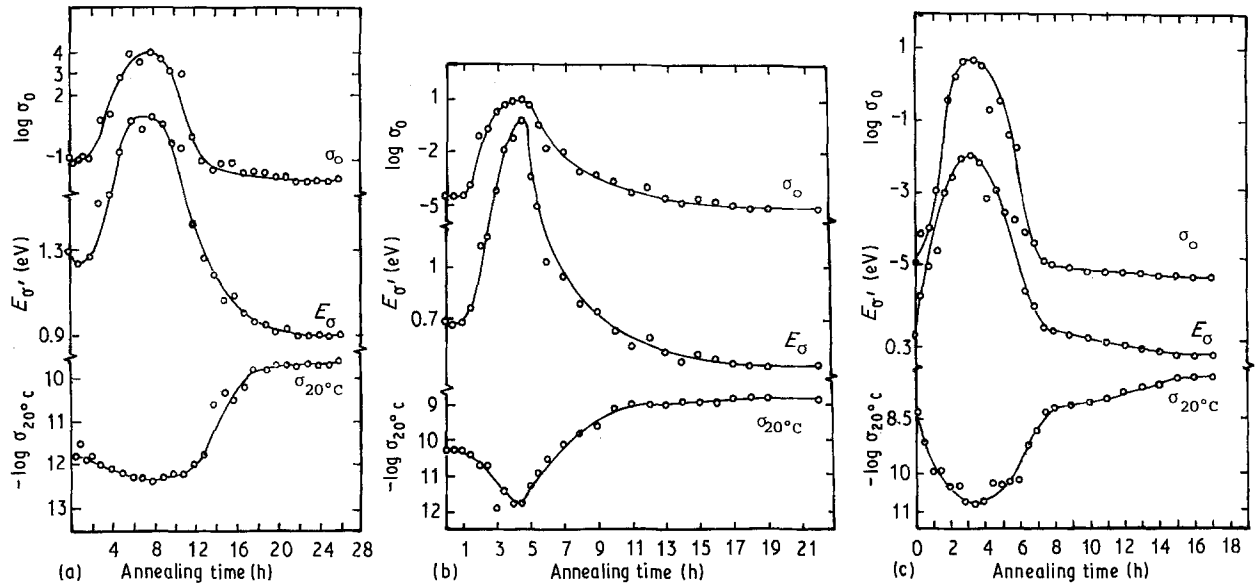

Figure 1 The annealing time-dependence of E_σ, $\sigma_{20°C}$ and σ_0 for glassy $Ag_x(As_2S_3)_{100-x}$ isothermally annealed at 200° C: x = (a) 6, (b) 15 and (c) 25.

formula

$$\sigma = \sigma_0 \exp(-E_\sigma/2KT)$$

Ageing of the glassy samples has been carried out in a preheated oven adjusted at a temperature lie between T_g and T_m of the glasses [8], namely 200° C. The linear relationship obtained for the function $\log \sigma = f(1/T)$ at the different stages of the amorphous–crystalline transformation indicate the semiconductor character of the investigated Ag–As_2S_3 materials whether in the glassy, crystal, or the intermediate states. The slopes of these straight lines increase at first with increasing the crystallization time for each composition, then they decrease until reaching a constant value, after which all the lines become almost parallel. From these lines, the values of the characteristic quantities activation energy of the conduction process (E_σ), specific electrical conductivity at 20° C ($\sigma_{20°C}$), and pre-exponential factor (σ_0) were obtained for each step of annealing.

The annealing time-dependence of E_σ, $\sigma_{20°C}$, and σ_0 are shown in Fig. 1 for the investigated compositions of the system $Ag_x(As_2S_3)_{100-x}$. These results indicate that the values of each of the electrical quantities E_σ, $\sigma_{20°C}$ and σ_0 suffer changes from a value corresponding to the initial amorphous state to a limiting value corresponding to the final crystallized mode. It is also clear that the time dependence of each quantity displays an induction period, decreases with increasing silver content, after which the change in property proceeds almost monotonically. The initial and final values of the investigated quantities, together with the duration of both induction and complete crystallization processes, are given in Table I as a function of composition.

The value of E_σ for the composition of $Ag_6(As_2S_3)_{94}$, for example, shows an increase from 1.29 to 1.9 eV after 8 h annealing at 200° C, then it decreases, reaching a constant value of 0.9 eV after 22 h annealing where the sample becomes crystallized, as indicated by its X-ray diffraction pattern. That is, E_σ suffers a decrease during the amorphous-crystalline transformation process at 200° C by $\approx 30\%$. Such a decrease in E_σ is accompanied by an increase in $\sigma_{20°C}$ by 19% and a decrease in σ_0 by 125%. A similar behaviour is observed for the other two compositions investigated. Table I indicates that increasing the silver content from 6 to 25 at % in the glasses of $Ag_x(As_2S_3)_{100-x}$ leads to a decrease in the time required to transfer the glassy phase into a crystallized one. That is, increasing the silver content leads to acceleration of the crystal growth in the compositions investigated.

3.2. Micrograph patterns of crystallization

Infrared and combination-scatter spectroscopy studies

TABLE I Results of the initial (amorphous) and final (crystalline) values of E_σ, $\sigma_{20°C}$ and σ_0 together with the induction and total crystallization periods for $Ag_x(As_2S_3)_{100-x}$ annealed at 200° C

Composition	Characteristic property	Initial value	Final value	Induction period (h)	Crystallization period (h)	Change (%) (approx.)
$Ag_6(As_2S_3)_{94}$	E_σ (eV)	1.29	0.90			30
	$-\log \sigma_{20°C}$	11.85	9.60	8	22	19
	$-\log \sigma_0$	0.80	1.80			125
$Ag_{15}(As_2S_3)_{85}$	E_σ (eV)	0.69	0.44			36
	$-\log \sigma_{20°C}$	10.32	8.80	4.5	18	15
	$-\log \sigma_0$	4.40	5.00			14
$Ag_{25}(As_2S_3)_{75}$	E_σ (eV)	0.38	0.24			37
	$-\log \sigma_{20°C}$	8.25	7.30	3.5	15	12
	$-\log \sigma_0$	4.90	5.25			7

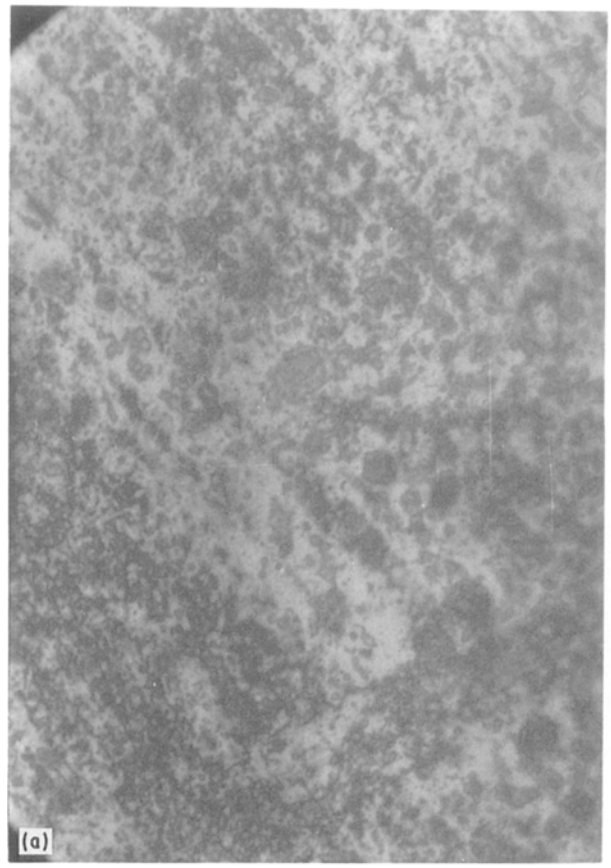

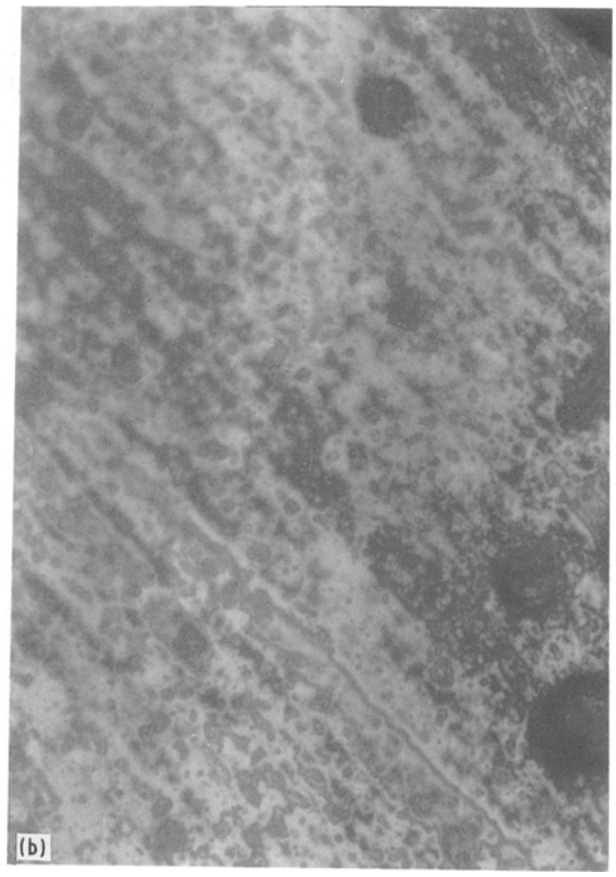

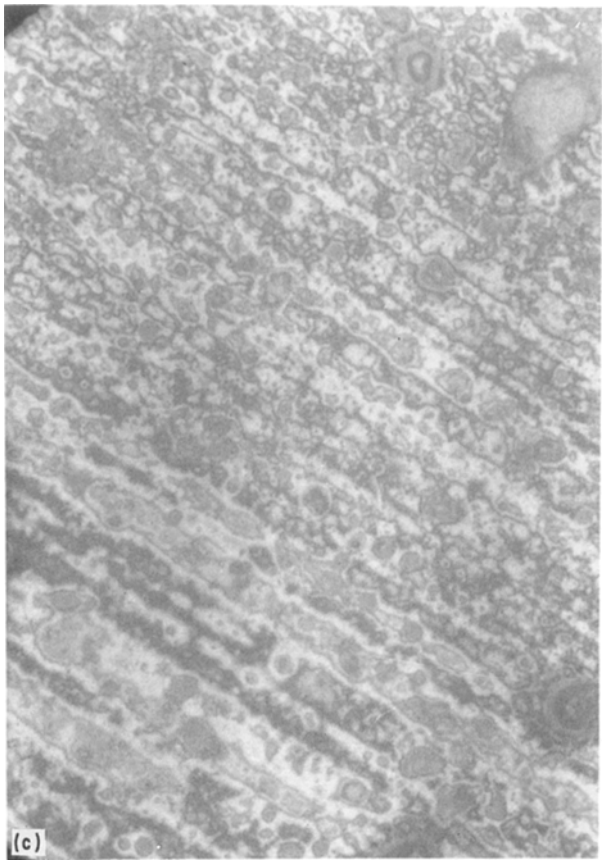

Figure 2 Reflection photomicrograph patterns taken for $Ag_6(As_2S_3)_{94}$ film ($\approx 100\,\mu m$) after isothermal annealing for different times at 200° C: (a) 1 h, (b) 2 h, (c) 5 h. The film was prepared by ice-quenching from the melt. ×315

by Golovach *et al.* [13] revealed the existence of the As_2S_3 and $AgAsS_2$ structural formations in Ag–As–S glasses. Hence, it was concluded that the glass-forming region in this system, in the structural sense, can be divided into two clearly defined and spatially differential parts: in one part, glasses based on As_2S_3 are formed and in the other, those on $AgAsS_2$; the glasses of both parts are characterized by great transparency and homogeneity. The glasses which in composition lie between the two parts of the glass-forming region are opalescent. The presence of opalescent glasses in the Ag–As–S system is associated with the process of stable or metastable demixing of the corresponding systems.

So, to follow the morphological changes in the investigated compositions, amorphous films of $\approx 100\,\mu m$ were isothermally annealed inside a pre-heated oven adjusted to 200° C. This temperature lies around the temperatures at which the crystallization started, as indicated from DTA measurements [8]. Selected micrograph patterns taken from the free-surface sides after annealing at different times are shown in Fig. 2 for $Ag_6(As_2S_3)_{94}$ ice-quenched from the melt, and in Fig. 4 for $Ag_{25}(As_2S_3)_{75}$ air-quenched from the melt. Fig. 3 shows those for the three investigated compositions taken after annealing the films for 4 h.

The tendency to form a texture with increasing annealing time is evident in Fig. 2 where the amorphous–crystalline transition passes through one metastable stage (single exothermic peak in DTA at $10°\,C\,min^{-1}$, [8]). The chains of the crystalline paths have spread almost over the whole surface of the $Ag_6(As_2S_3)_{94}$ film after annealing for 5 h.

The photomicrographs of Fig. 3 indicate that the increase of the concentration of silver atoms greatly

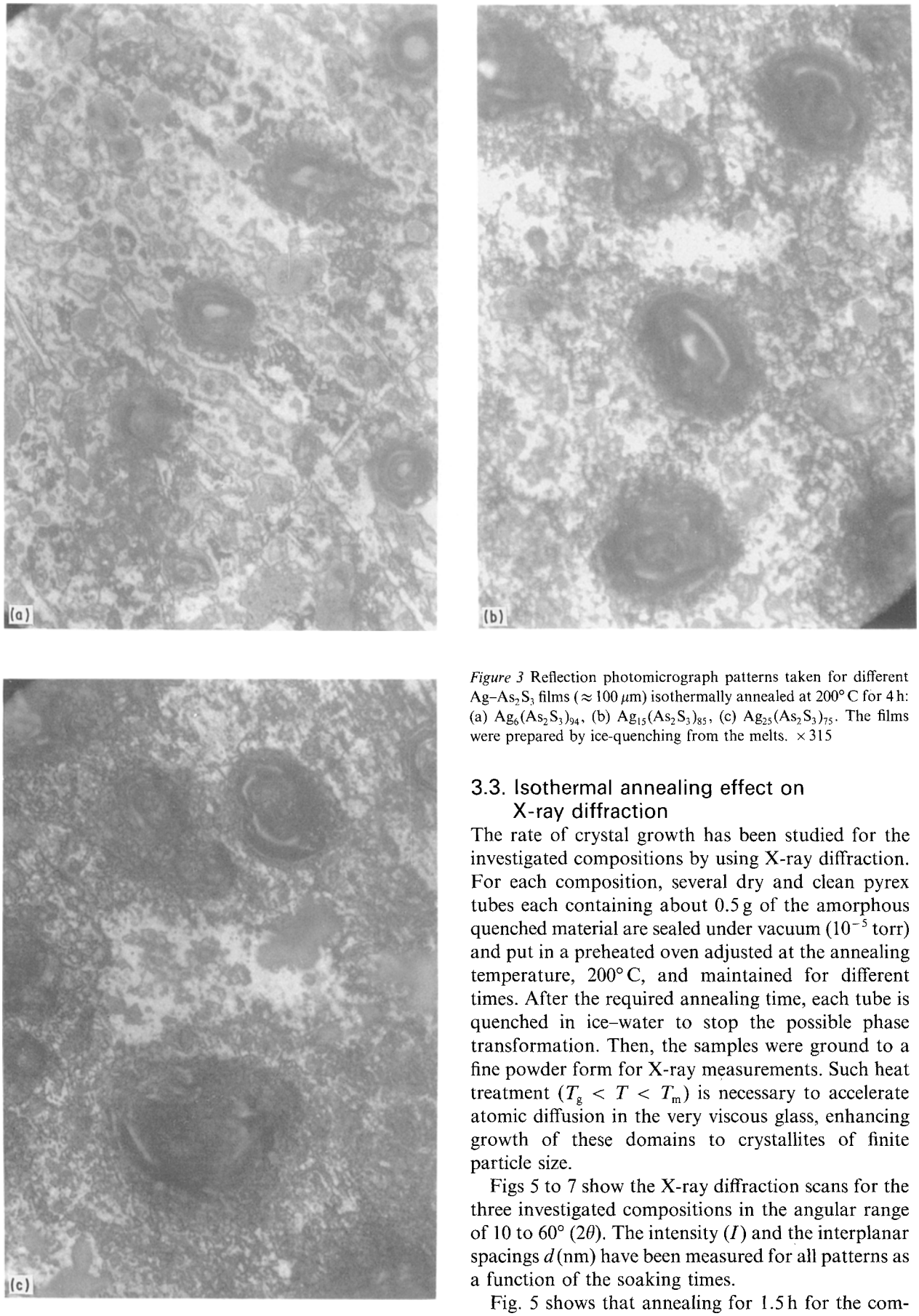

Figure 3 Reflection photomicrograph patterns taken for different $Ag–As_2S_3$ films ($\approx 100\,\mu m$) isothermally annealed at 200° C for 4 h: (a) $Ag_6(As_2S_3)_{94}$, (b) $Ag_{15}(As_2S_3)_{85}$, (c) $Ag_{25}(As_2S_3)_{75}$. The films were prepared by ice-quenching from the melts. × 315

affects the size and formation of spherulites embedded in amorphous zones due to heterogeneous nucleation.

Of course, the rate of quenching plays another role in affecting the rate of crystal growth. Fig. 4 shows the effect of annealing time on the texture of $Ag_{25}(As_2S_3)_{75}$ film prepared by air-quenching from the melt.

3.3. Isothermal annealing effect on X-ray diffraction

The rate of crystal growth has been studied for the investigated compositions by using X-ray diffraction. For each composition, several dry and clean pyrex tubes each containing about 0.5 g of the amorphous quenched material are sealed under vacuum (10^{-5} torr) and put in a preheated oven adjusted at the annealing temperature, 200° C, and maintained for different times. After the required annealing time, each tube is quenched in ice–water to stop the possible phase transformation. Then, the samples were ground to a fine powder form for X-ray measurements. Such heat treatment ($T_g < T < T_m$) is necessary to accelerate atomic diffusion in the very viscous glass, enhancing growth of these domains to crystallites of finite particle size.

Figs 5 to 7 show the X-ray diffraction scans for the three investigated compositions in the angular range of 10 to 60° (2θ). The intensity (I) and the interplanar spacings d (nm) have been measured for all patterns as a function of the soaking times.

Fig. 5 shows that annealing for 1.5 h for the composition $Ag_6(As_2S_3)_{94}$ leads to the appearance of six diffraction lines, including the line of $d = 0.3640$ nm, which represent the 100% line in the complete crystalline matrix. Increasing the time of annealing to 4 h leads to the appearance of the line of $d = 0.2427$ nm [9]. Further annealing at 200° C leads to the gradual appearance of the other diffraction lines characterizing

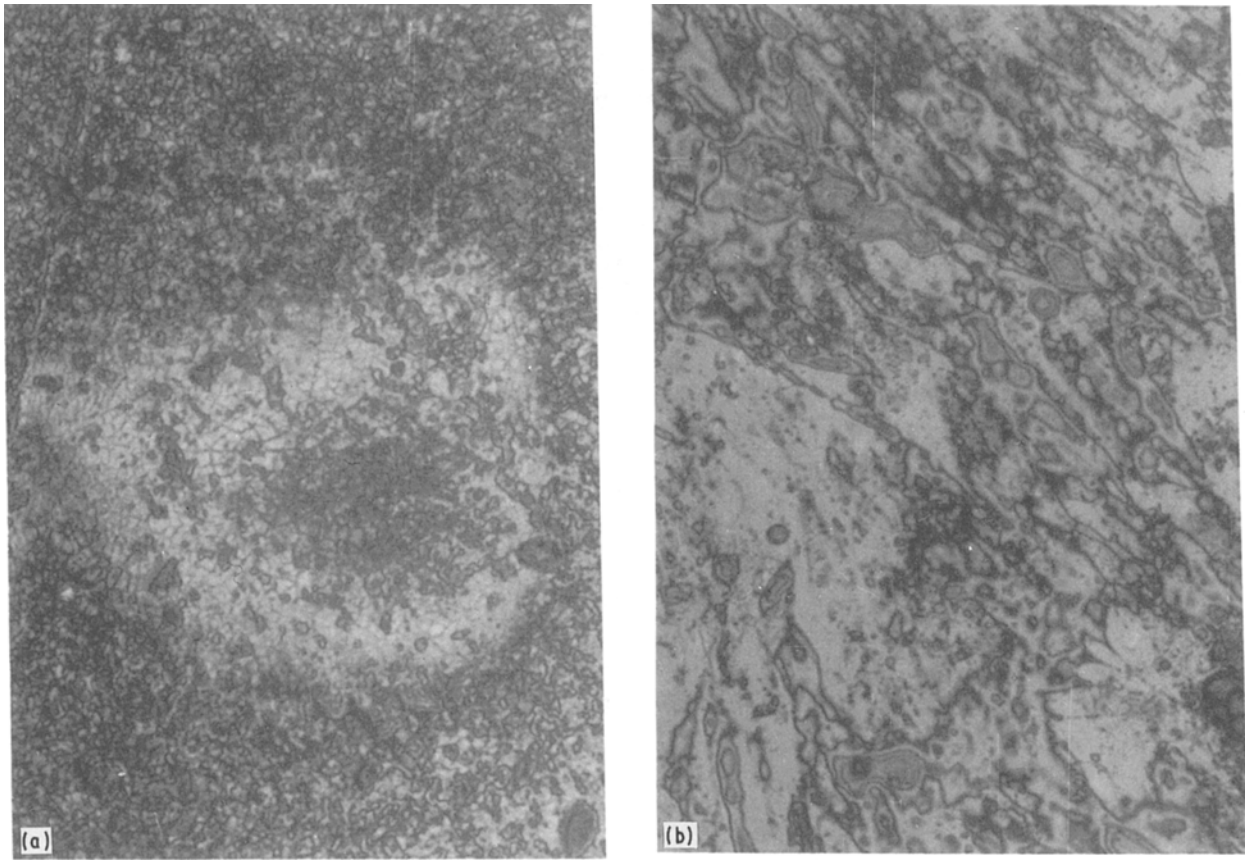

Figure 4 Reflection photomicrograph patterns taken for $Ag_{25}(As_2S_3)_{75}$ film ($\approx 100\,\mu m$) after isothermal annealing for different times at 200° C. (a) As-prepared, (b) 3 min, (c) 12 min. The film was prepared by air-quenching from the melt. ×315

the crystalline structure of the composition investigated. The intensity of the lines is slightly increased with increasing the annealing.

Fig. 6 shows three diffraction lines at $d = 0.769$ nm (6), 0.367 nm (18) and 0.3002 nm (17) when annealing the glass $Ag_{15}(As_2S_3)_{85}$ for 30 min (the numbers in parentheses represents the intensity of the diffraction line). Other diffraction lines such as 0.4087 nm (23), 0.3445 nm (12), 0.243 nm (15), 0.2021 nm (12), 0.181 nm (15) start to appear after annealing for 3 h. Annealing at 200° C for 8 h leads to the appearance of different new lines. The rest of the diffraction pattern characterizes the composition of $Ag_{15}(As_2S_3)_{85}$, which is present in the pattern at the top of the figure. The intensity of the lines as well as the relative half-width of the peaks change randomly for some of the reflections with increasing annealing time, indicating preferred orientation for some planes.

The effect of annealing time on the X-ray diffraction patterns for the composition $Ag_{25}(As_2S_3)_{75}$ indicates that 15 min annealing at 200° C is not sufficient to detect any diffraction lines. However, six diffraction lines appeared after annealing for 30 min. These lines are of $d = 0.3640$ nm (3), 0.3130 nm (6), 0.2705 nm (1), 0.234 nm (1), 0.194 nm (2), and 0.1879 nm (2). The rest of the diffraction pattern characterizes the crystalline structure of this composition appeared after annealing for almost 1.5 h.

3.4. Structural changes with composition

The material which had been found to be in the amorphous phase by the quenching technique was subjected to an annealing process at 200° C for about 20 h, and then allowed to cool slowly in the oven. This was done to obtain samples in the crystalline

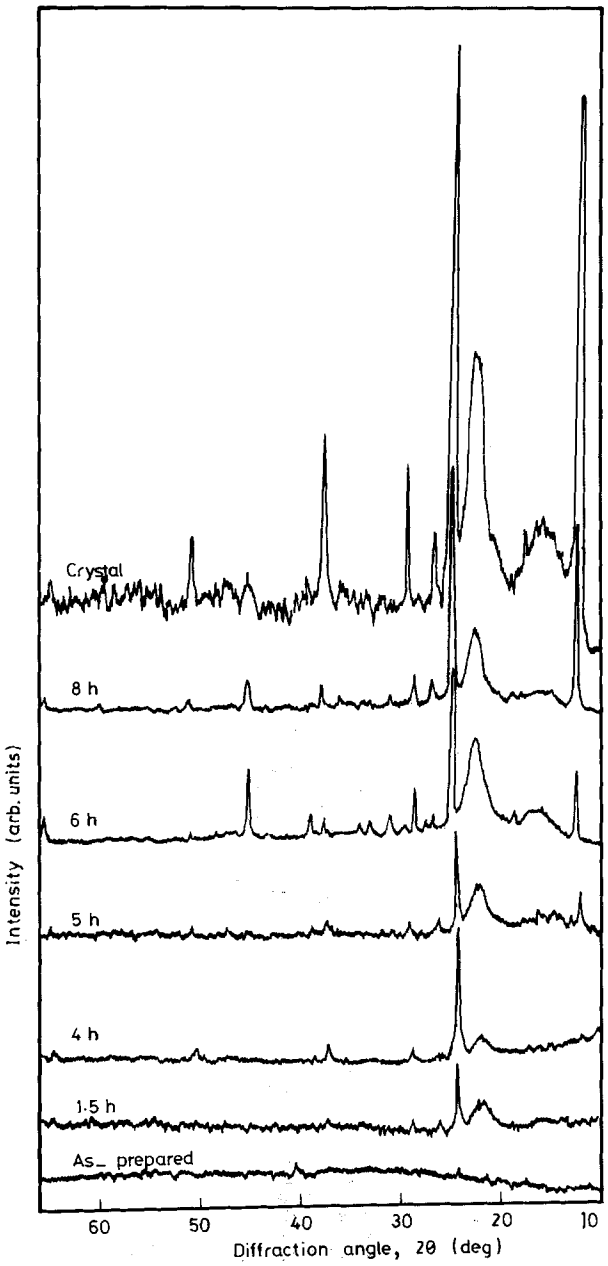

Figure 5 X-ray diffraction patterns of $Ag_6(As_2S_3)_{94}$ annealed at 200° C for different times.

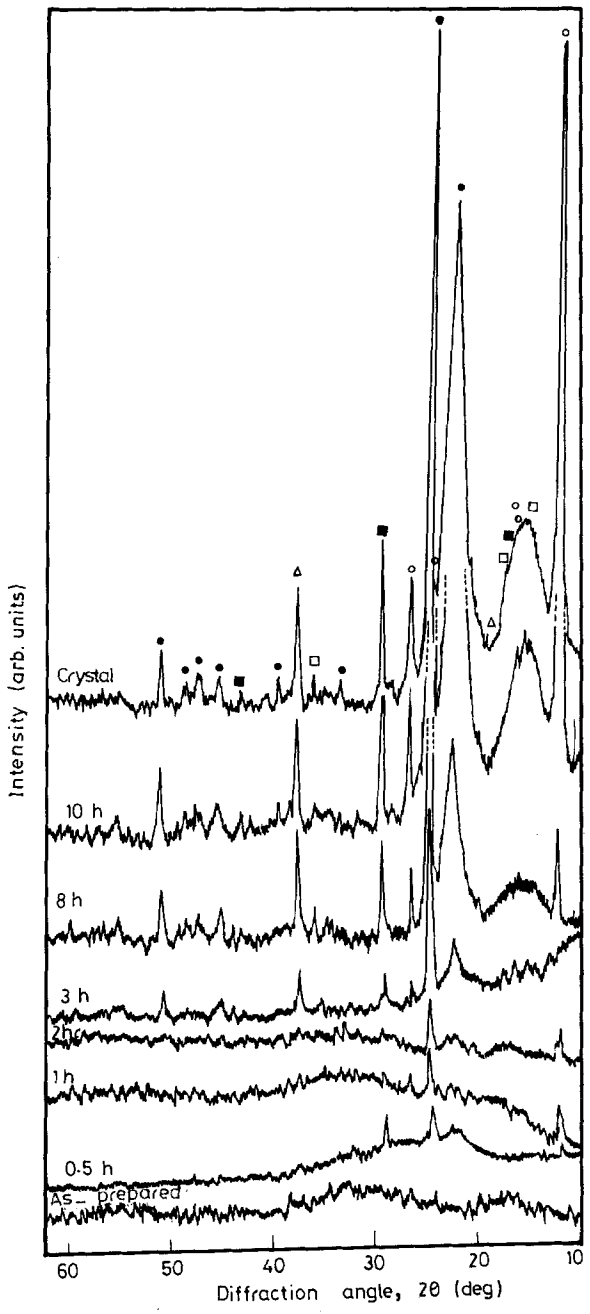

Figure 6 X-ray diffraction patterns of $Ag_{15}(As_2S_3)_{85}$ annealed at 200° C for different times. (○) S, (□) AsS, (●) $AgAs_2S_2$, (■) $Ag_6As_2S_6$, (△) As_2S_3.

state. These were prepared in powder form for X-ray analysis.

A comparison of the data obtained for the interplanar spacings (d_{hkl}) and their corresponding relative intensities (I/I_0%) of the three investigated compositions with those given in the ASTM Diffraction State File Index for the parents As_2S_3 and silver and those of the other probabilities; sulphur, AsS, $AgAs_2S_2$ and $Ag_6As_2S_6$, indicates that the effect of addition of silver to As_2S_3 is accompanied by different changes, some of which are great, in the diffraction patterns, Table II. These changes appear as a shift in the position, change in intensity of some lines and the presence of new lines. The latter represent the character of the diffraction patterns of the compositions investigated. That is, only a few lines of the parent As_2S_3 still exist after addition of silver. These lines are d = 0.4803 nm (14%) for the composition of 6 at % Ag; d = 0.4805 nm (6%) and 0.2429nm (23%) for the composition of 15 at % Ag; and nothing appeared for As_2S_3 in the composition of $Ag_{25}(As_2S_3)_{75}$. Some strong lines for elemental sulphur appeared in the diffraction patterns of the three Ag–As_2S_3 compositions. The intensity of the S-lines changes between 5 and 100%. Most of the diffraction lines of the composition $Ag_6(As_2S_3)_{94}$ belong to the phase $AgAs_2S_2$ and three lines of d = 0.6114 nm (14%), 0.5399 nm (14%) and 0.2020 nm (9%) belong to the phase AsS. Comparing the intensity of the different lines of the different phases forming the solid solution of $Ag_6(As_2S_3)_{94}$ with those in the ASTM cards indicates a preferred orientation of the planes for most phases.

Increasing the concentration of silver in the compound to 15 at % leads to the appearance of three new lines belonging to the phase $Ag_6As_2S_6$. These lines are of d = 0.5503 nm (17%), 0.3004 nm (26%) and 0.2132 nm (5%). The second line represents the 100% line in the structure of $Ag_6As_2S_6$. The four phases S,

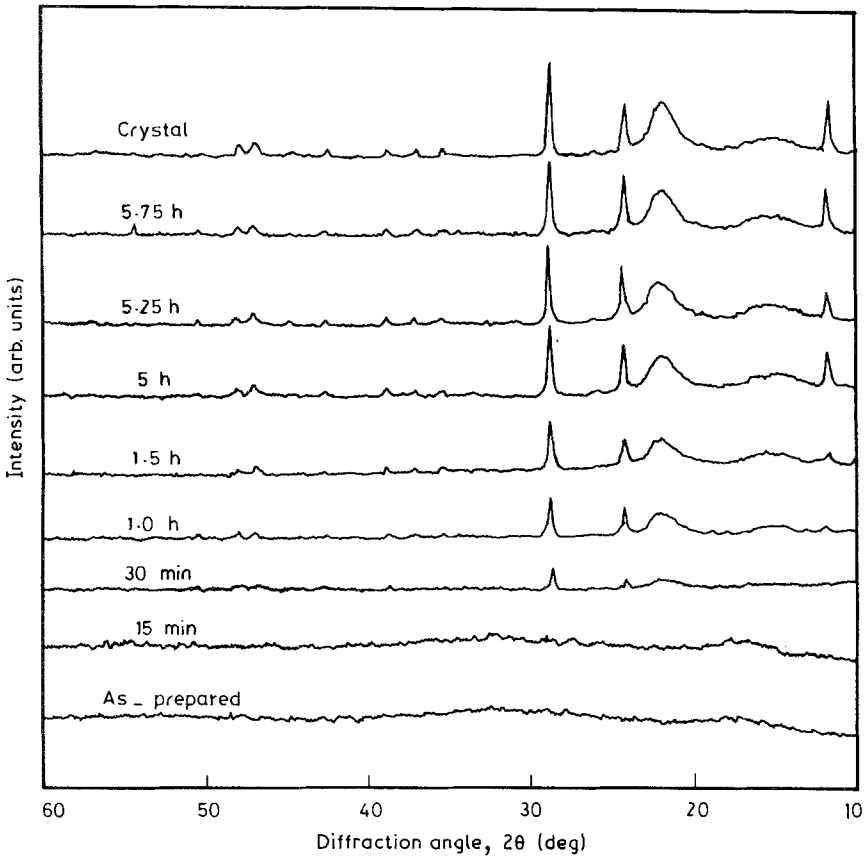

Figure 7 X-ray diffraction patterns of $Ag_{25}(As_2S_3)_{75}$ annealed at 200°C for different times.

TABLE II Interplanar spacings and relative intensities of polycrystalline $Ag_x(As_2S_3)_{100-x}$ together with the identification phases

$Ag_6(As_2S_3)_{94}$		$Ag_{15}(As_2S_3)_{85}$		$Ag_{25}(As_2S_3)_{75}$		Proposed composition	Identification		*hkl*	ASTM no. [references]
d (nm)	I/I_0	*d* (nm)	I/I_0	*d* (nm)	I/I_0		*d* (nm)	I/I_0		
0.7693	87	0.7690	81	0.7692	52	S	0.7690	6	111	(8-247), [14]
0.7003	12					$AgAs_2S_2$	0.7000	60	110	(16-700), [17]
0.6114	14	0.6110	18			AsS	0.6110	20	$\bar{1}01$	(9-441), [15]
0.5761	12	0.5764	17			S	0.5760	14	113	(8-247), [14]
0.5682	13	0.5684	16			S	0.5680	5	022	(8-247), [14]
		0.5503	17			$Ag_6As_2S_6$	0.5500	20	202, $\bar{1}11$, 111	(8-134), [18]
0.5399	14	0.5402	16			AsS	0.5400	100	$\bar{1}11$, 120	(9-441), [15]
0.4803	14	0.4805	6			As_2S_3	0.4800	100	020	(24-75), [16]
0.4092	40	0.4090	80	0.4092	44	$AgAs_2S_2$	0.4090	30	121	(16-700), [17]
0.4060	45					S		11	220	(8-247), [14]
0.3851	45	0.3853	18	0.3849	40	S		100	222	(8-247), [14]
0.3641	100	0.3640	100	0.3641	50	$AgAs_2S_2$	0.3640	60	022	(16-700), [17]
0.3493	12					$AgAs_2S_2$		5	220	(16-700), [17]
		0.3439	23			S	0.3440	40	026	(8-247), [14]
				0.3379	5	S	0.3380	3	224	(8-247), [14]
0.3150	4					$AgAs_2S_2$	0.3150	80	311	(16-700), [17]
0.3109	27			0.3110	100	S	0.3110	25	313	(8-247), [14]
		0.3004	26			$Ag_6As_2S_6$	0.3000	100	400, $\bar{1}19$, $\bar{3}15$, 119, 315	(8-134), [18]
0.2701	5	0.2702	5	0.2704	9	$AgAs_2S_2$	0.2702	100	142	(16-700), [17]
		0.2604	5			AsS	0.2600		150, 032	(9-441), [15]
0.2522	5					$AgAs_2S_2$	0.2520	10	402	(16-700), [17]
		0.2429	23			As_2S_3	0.2429	100	330, 420	(24-75), [16]
				0.2424	8	$AgAs_2S_2$	0.2424	10	303	(16-700), [17]
0.2404	31					S	0.2404	2	404	(8-247), [14]
0.2328	7	0.2327	5	0.2327	8	$AgAs_2S_2$	0.2329	20	330	(16-700), [17]
		0.2132	5			$Ag_6As_2S_6$	0.2130	30	$\bar{2}.0.14$, 2.0.14	(8-134), [18]
0.2020	9					AsS	0.2020	10		(9-441), [15]
		0.2016	8			$AgAs_2S_2$	0.2018	5	600	(16-700), [17]
0.1938	7	0.1936	7	0.1938	7	$AgAs_2S_2$	0.1937	70	520	(16-700), [17]
0.1887	6	0.1888	5	0.1886	12	$AgAs_2S_2$	0.1887	80	314	(16-700), [17]
0.1806	18	0.1805	17			$AgAs_2S_2$	0.1807	5	611, 105	(16-700), [17]
0.1575	5					$AgAs_2S_2$	0.1576	50	622	(16-700), [17]
0.1419	7					$AgAs_2S_2$	0.1420	5	306	(16-700), [17]

As_2S_3, AsS and $AgAs_2S_2$ appearing in the composition of 6 at % Ag are still present in the composition of 15 at % Ag, retaining the preferred orientation for some phases, such as those of $d = 0.7690$ nm (S), 0.4090 nm ($AgAs_2S_2$) and 0.3640 nm ($AgAs_2S_2$).

For the composition of 25 at % Ag, the lines of the three phases AsS, As_2S_3 and $Ag_6As_2S_6$ disappeared. The diffraction pattern of this composition is very simple and contains only lines corresponding to the two phases S and $AgAs_2S_2$, retaining the preferred orientation. The lines of the S-phase are those of $d = 0.7692$ nm (52%), 0.3849 nm (40%), 0.3379 nm (5%) and 0.3110 nm (100%). Also, the lines of the $AgAs_2S_2$-phase are those of $d = 0.4092$ nm (44%), 0.3641 nm (50%), 0.2704 nm (9%), 0.2424 nm (8%), 0.2327 nm (8%), 0.1938 nm (7%) and 0.1886 nm (12%). That is, the structure of the composition of $Ag_{25}(As_2S_3)_{75}$ may be represented as a solid solution of elementary and ternary systems, S and $AgAs_2S_2$.

4. Conclusions

A study of the effects of the addition of silver on the electrical conduction and isothermally induced transition of amorphous arsenic trisulphide, As_2S_3, at $T_g < T < T_m$ allows us to draw the following conclusions.

1. The d.c. conductivity is a sensitive measurable parameter by which to follow the induced structural changes in the Ag–As_2S_3 glasses. The semiconducting character of the samples is preserved whether in the initial glassy, crystal, or in the intermediate stages. The amorphous–crystalline transition is accompanied by a decrease in E_σ (30 to 37%), an increase in $\sigma_{20°C}$ (12 to 19%), and a decrease in σ_0 (7 to 125%). The rate of change is monotonic with silver content.

2. The increase of silver content in the sample leads to acceleration of the rate of crystal growth in the amorphous matrix.

3. The structure of the three-component system $Ag_x(As_2S_3)_{100-x}$ can be represented as a solid solution of S, AsS, $AgAs_2S_3$ and As_2S_3 for the composition of $x = 6$; S, AsS, $AgAs_2S_2$, $Ag_6As_2S_6$ and As_2S_3 for $x = 15$; and the solid solution for $x = 25$ only consists of two phases, S and $AgAs_2S_2$.

References

1. K. S. LIANG, A. BIENENSTOCK and C. W. BATES, *Phys. Rev.* **B10** (1974) 1528.
2. N. F. MOTT, E. A. DAVIS and R. A. STREET, *Phil. Mag.* **32** (1975) 961.
3. R. MANAILA and M. POPESCU, Personal communication at the Conference of Amorphous, Liquid and Vitreous Semiconductors, Sofia (1972).
4. D. GOLDSCHMIDT, 4th International Conference on the Physics of Non-Crystalline Solids, Clausthal, Germany, September 1976.
5. S. R. FRITZCHE and S. R. OVSHINSKY, *J. Non-Cryst. Solids* **2** (1970) 148.
6. K. TANAKA, S. LIZIMA, M. SUGI, Y. OKATA and M. KIKUCHI, *Solid State Commun.* **8** (1970) 1333.
7. M. P. KIT, M. T. KOSTYSHIN, K. S. MUSTAFIN, P. F. ROMANEKO and V. A. SELEZNEV, *Sov. J. Quantum Electron.* 7 (1977) 47.
8. M. F. KOTKATA, M. M. RADWAN, F. M. METAWE and C. S. MOHAMED, *J. Non-Cryst. Solids* **77/78** (1985) 1229.
9. M. M. RADWAN, PhD thesis, University of Dundee (1982).
10. C. S. MOHAMED, MSc thesis, University of Ain Shams, Cairo, Egypt (1987).
11. M. F. KOTKATA and A. F. EL-DIB, *Mater. Sci. Engng* **67** (1984) 39.
12. M. F. KOTKATA, H. H. LABIB and S. A. RAHMAN, *J. Thermal Anal.* **34** (1988) 93.
13. I. I. GOLOVACH, V. S. GERASIMENKO, V. YU. SLIVKA, N. I. DOVGOSHEI, A. V. BOGDANOVA and M. I. GOLOVEI, *Sov. J. Glass Phys. Chem.* **5** (1977) 430.
14. DEWOLF, "Techn. Phys." (Dienst, Delft, Holland, 1970).
15. AM. BUEREGER, *Min. Mag.* **20** (1935) 36.
16. TIMOFEEVA et al., Dokl. Phys. Chem. **190** (1970) 115.
17. British Museum (Natural History) London, UK.
18. PEACOCK, *Min. Mag.* **29** (1950) 346.

Received 10 February
and accepted 13 June 1988